

Multifunctional triboelectric nanogenerator based on porous micro-nickel foam to harvest mechanical energy

Lei Zhang, Long Jin, Binbin Zhang, Weili Deng, Hong Pan, Junfeng Tang, Minhao Zhu, Weiqing Yang*

Key Laboratory of Advanced Technologies of Materials (Ministry of Education), School of Materials Science and Engineering, Southwest Jiaotong University, Chengdu 610031, China

Received 24 May 2015; received in revised form 18 June 2015; accepted 18 June 2015
Available online 2 July 2015

KEYWORDS

Triboelectric nano-generator;
Porous micro-nickel foam;
Vibration energy;
Footfall;
Self-powered

Abstract

To strengthen the effective contact area of two materials with the opposite triboelectric polarities was proved to be an effective solution to enhance the electronic output of triboelectric nanogenerator (TENG). Presently, that mainly focused on the surface modification of negative materials by micro/nano structure, however, rarely for the positive materials. Here, we presented a simple, low-cost and multifunctional TENG based on the porous micro-nickel foam (PMNF) for harvesting the natural vibration energy. With the surface modification of PMNF with the positive polarity, the newly designed TENG produced an open-circuit voltage up to 187.8 V and a short-circuit current of 71.9 μA with the peak power density of 3.7 W/m^2 at the resonance frequency of 13.9 Hz by harvesting vibration energy. This TENG could simultaneously and continuously light up 100 commercial light-emitting diode bulbs. Additionally, by the footfalls force of about 500 N, the corresponding open-circuit voltage and short-circuit current were as high as 403 V and 336 μA , respectively. The newly designed TENG can be used for the self-powered floor by footfalls and also for powering some wireless electronics by harvesting the vibration energy from highways, railways, and tunnels in remote mountain areas.
© 2015 Elsevier Ltd. All rights reserved.

Introduction

In the past few years, many research efforts have been devoted to harvest ambient mechanical energy as the supplementation of traditional power source owing to the

increasingly less fossil fuels and the rapid-growing energy consumptions. Usually, several mechanisms on harvesting mechanical energy are as follows: electrostatic effect [1–5], piezoelectric effect [6–10], electromagnetic effect [11–13] and magnetostrictive effect [14]. Based on them, these methods mainly focused on the small-scale energy harvesting, intending to power micro/nanosystems and portable electronics [15–24] because of their small size, lower power

*Corresponding author.

consumption and special working environment. However, these widespread techniques toward large-scale energy harvesting are potentially shadowed by some possible restrictions, such as the energy harvesting method, the material cost [25], structural complexity [15], environmental influence and feasibility in practice.

The triboelectric effect, which has been known for thousands of years, was an undesirable phenomenon in past years owing to the potential threats to public safety and electric product. However, triboelectric nanogenerators [26–36] (TENGs), on this basis, has been hatched up to harvest mechanical energy as an efficient means. In virtue of coupling effect of contact electrification and electrostatic induction, the periodic contact and separation between two materials with triboelectric polarities could drive the charges between electrodes to produce an alternating current. The dramatically increasing effective contact area of contact materials by the micro/nano structure surface modification technique was proved to be one of the most important factors to strengthen the electronic output of TENG. Currently, only a few surface modification of positive materials by micro/nano structure [34] has been reported to date. The overwhelming majority of TENGs focused on the surface modification of positive materials [37–40].

Here in this paper, for the first time, a kind of low-cost, stable and porous micro-nickel foam (PMNF) with the positive property was applied to fabricate a TENG that can harness ambient vibration and footfalls, which are the most common and available mechanical motion for powering electronics, especially portable devices. With the hybridization [41–46] of both the contact-separation mode and sliding electrification mode of PMNF top inserting into flexible PDMS, the reasonably designed TENG can generate a uniform signal output at a short-circuit of 71.9 μA and an open-circuit voltage up to 187.8 V, which corresponded to the power output of 9.3 mW and power density of 3.7 W/m². Additionally, by the footfalls force of about 500 N, the corresponding open-circuit voltage and short-circuit current are up to respectively 403 V and 336 μA , which unambiguously presented some potential applications of PMNF for the, self-powered floor and anti-theft devices as well as vibration sensor system by harvesting the vibration energy from highways, railways, and tunnels in remote mountain areas.

Results and discussion

Figure 1a illustrates the schematic diagram of TENG that consists of two substrates, electrodes, triboelectric materials and springs. Acrylic was selected as supporting substrate in virtue of its felicitous strength with good processing, light weight, graceful appearance and low cost. As the as-fabricated TENG schematically shown in Figure 1b, a sheet of porous PMNF that has dual roles as a contact surface and an electrode was attached on the lower side. This porous electrode was prepared via an electrolytic-deposition method, which will be discussed in details in the *Experimental section*. A scanning electron microscopy (SEM) image of PMNF sketched in Figure 1c. In addition, the corresponding energy dispersive spectrometer (EDS) is presented in

Figure S1. On the other side, a thin layer of aluminum foil, called back electrode, was fixed on the substrate and the polydimethylsiloxane (PDMS) as contact surface directly spin-coated on it. Then, four springs support the two substrates remaining a narrow gap at the corners. Figure 1d distinctly schemes the fabrication flow and the concrete fabrication process is describe in detail later.

The working principle of this nanogenerator can be expounded as schematically depicted in Figure S2 by means of the triboelectric effect and electrostatic effect. The electricity generation process in this TENG is based on the sequence of contact-separation motion induced by a standard vibration shaker system (from Dongling Technologies Inc.). When an external force from the vibration shaker system gives rise to the contact, an electrical signal distinct is obtained by the contact and sliding mode of the TENG. Subsequently, with the separation achieved up until the maximal point, the inductive charges gradually transfer from PMNF to PDMS's back electrode [46]. In addition, when the two contact surfaces narrow the interval of two contact surfaces until contact, an electric potential difference is produced once again and free electrons flow back to PMNF. In this process, the TENG is similar to an electric pump that drives electrons back and forth between electrodes, producing an alternating current. Furthermore, in order to reinforce the working principle, we took a further step to simulate the periodic potential change between the two electrodes upon vertical contact and separation by virtue of COMSOL, as demonstrated in Figure 2. And the continuous variation of the potential distribution is visualized in Supporting information Movie 1.

Supplementary material related to this article can be found online at <http://dx.doi.org/10.1016/j.nanoen.2015.06.012>.

In order to investigate the performance of TENG for harvesting vibration energy [20], the standard vibration shaker system as a vibration source supplied an adjustable frequency and amplitude in form of a sine-wave oscillation. The bottom substrate of TENG was fixed on the shaker, making sure that this TENG should be on the safe side and its upper part can run free. The peak value of open-circuit voltage (V_{oc}) and short-circuit current (I_{sc}) as functions of input vibration frequencies at an invariable amplitude were measured in Figure 3a and b to characterize the TENG electric performance. A far-ranging common vibration frequency in daily was surveyed from 1 to 300 Hz in a super-low-frequency (SLF) scale (Table 1, Supporting information). And a considerably wider working bandwidth of 11.2 Hz was obtained (see Figure S3, Supporting information).

Experimentally, the open-circuit voltage and the short-circuit current of TENG reached the maximum values of respectively 187.8 V and 71.9 μA at the vibration frequency of 13.9 Hz, revealing that 13.9 Hz should be the resonance frequency of TENG. In theory, for a degree-of-freedom vibration system, the natural is given by the following equation [47]:

$$f_0 = \frac{1}{2\tau} \sqrt{\frac{4k}{m_0}} \quad (1)$$

where f_0 is the natural frequency, k is the stiffness coefficient is 132 N m⁻¹ and m_0 is 69 g for the TENG. We can acquire the nature frequency of 13.9 Hz by inputting

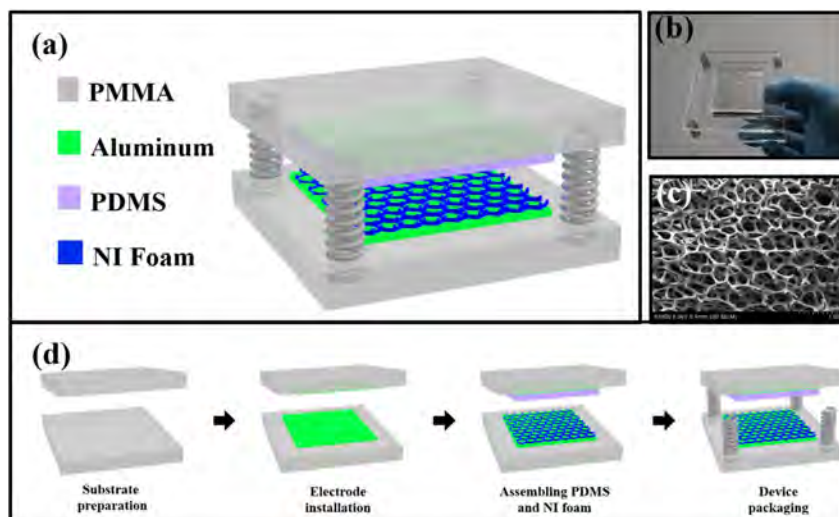


Figure 1 Porous micro-nickel foam based triboelectric nanogenerator. (a) Schematic and (b) photograph of a fabricated TENG. (c) An SEM image of porous micro-nickel foam. (d) Process flow for fabricating the porous nickel foam based TENG.

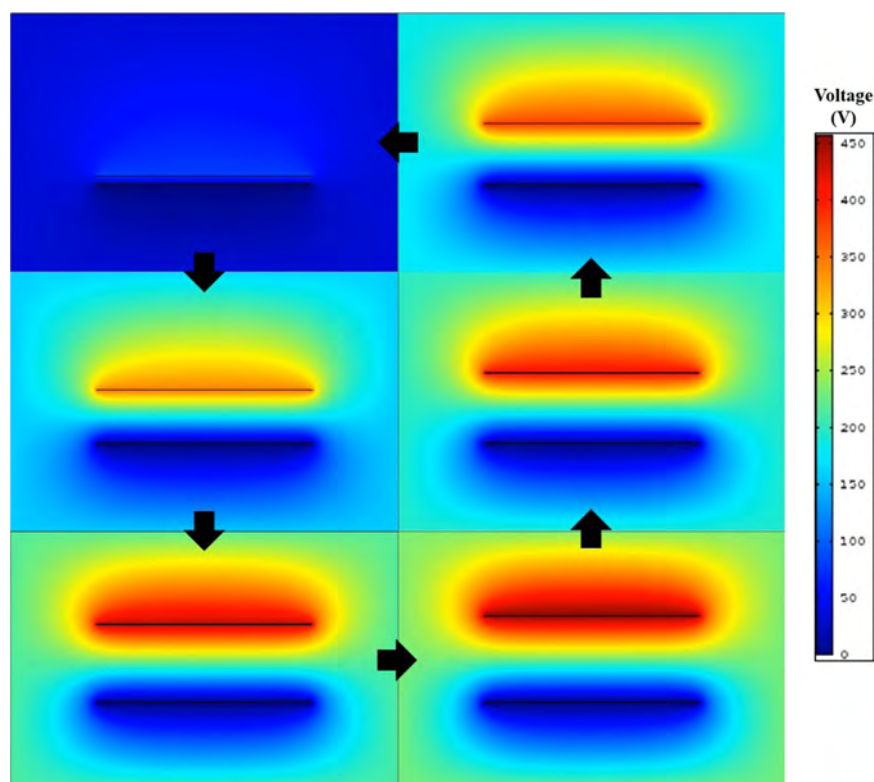


Figure 2 Finite-element simulation of the potential distribution in the device in a contact-separate-contact cycle.

the values into Eq. (1), which coincides with the experimental result.

At the resonance frequency of 13.9 Hz, the open-circuit voltage is elaborated in Figure 3c. Since the upper substrate of TENG vibrates in a unified quasi-sinusoidal way, it presents an analogous signal. Theoretically, this TENG can be considered as a damped system subjected to a harmonically varying force. Hence, the maximum V_{oc} at the resonance frequency can be demonstrated as (see Supporting information for detailed derivation of the analytical model)

$$V_{oc-rf} = \frac{\sigma}{\epsilon_0} \cdot \frac{m_0 a}{2k\xi} \quad (2)$$

where ϵ_0 is the vacuum permittivity ($8.854 \times 10^{-12} \text{ F m}^{-1}$), σ is the triboelectric charge density ($0.003016 \mu\text{C cm}^{-2}$ (Figure S4, Supporting information), ξ is the damping factor of the TENG system (0.354 by experimental measurement, in Figure S5, Supporting information) and a is the acceleration of the standard vibration shaker system (a typical value of $g/50$ where g is the gravitational

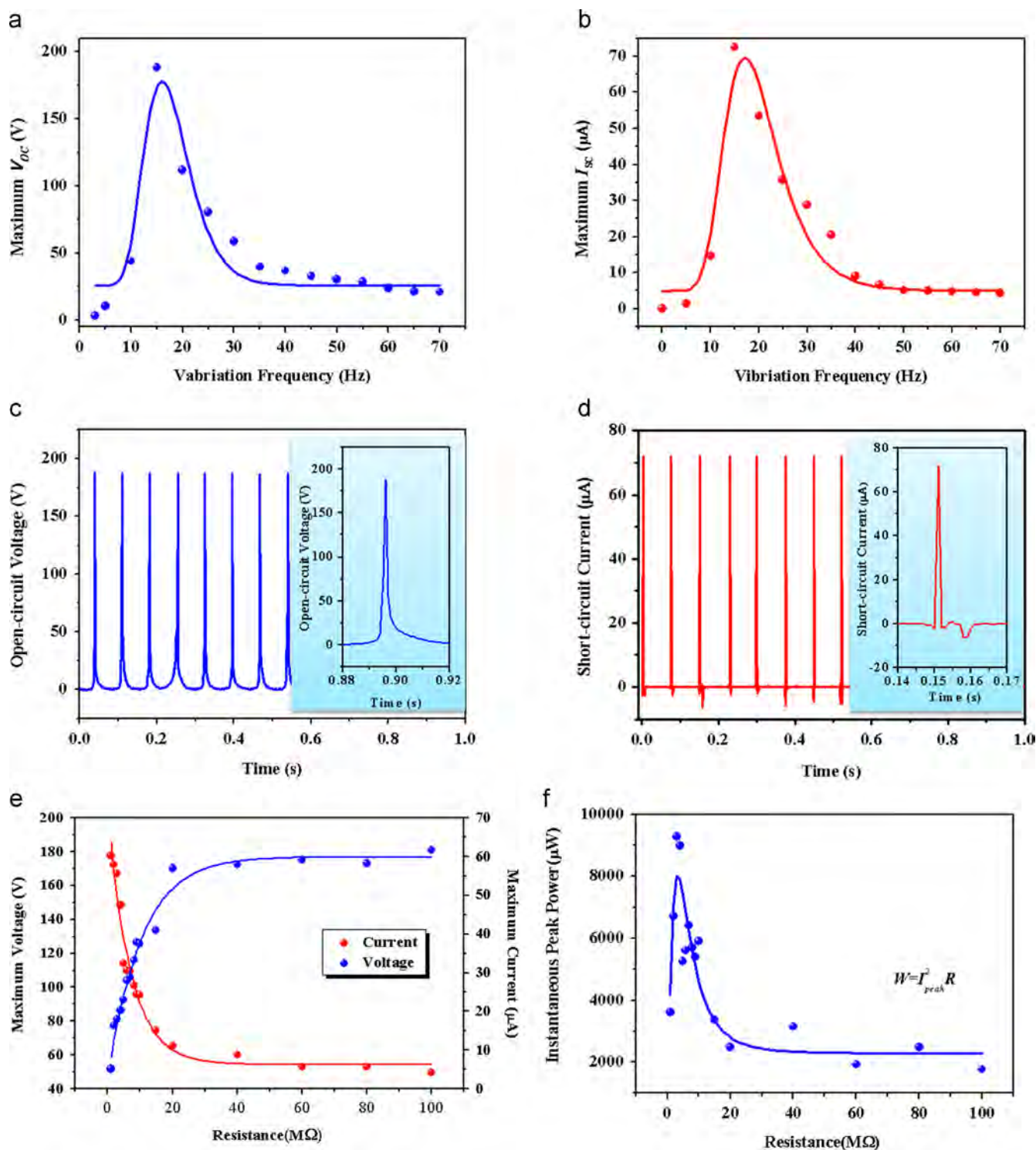


Figure 3 Electrical measurement results of the TENG. (a) Open-circuit voltage (V_{oc}) as a function of vibration frequency. The curve is a fitted result. (b) Short-circuit current (I_{sc}) as a function of vibration frequency. The curve is a fitted result. (c) Open-circuit voltage (V_{oc}) at harmonic-resonator vibration frequency of 13.9 Hz. Inset: enlarged view of one cycle. Separation causes rising of the V_{oc} to a peak value and contact make it fall back to zero. (d) Short-circuit current (I_{sc}) at harmonic-resonator vibration frequency of 13.9 Hz. Inset: enlarged view of one cycle. Contact and separation correspond to a positive current pulse and a negative current pulse, respectively, presenting an alternating-current (AC) characteristic; (e) Dependence of the voltage and current output on the external load resistance. The points represent peak value of electric signals while the lines are the fitted results; (f) Dependence of the peak power output on the resistance of the external load, indicating maximum power output when $R=3 M\Omega$. The curve is a fitted result.

acceleration). According to the theoretical calculation in Eq. (2), the peak value of V_{oc} is up to 492.9 V larger than the experimental result of 187.8 V. This difference probably results from the assumptions made in the analytical model

and non-ideal factors in the experiment, such as a little bit moisture-laden air and the imbalance of vibration.

In Figure 3d, the short-circuit current at the resonance frequency manifests an asymmetrical-amplitude alternating

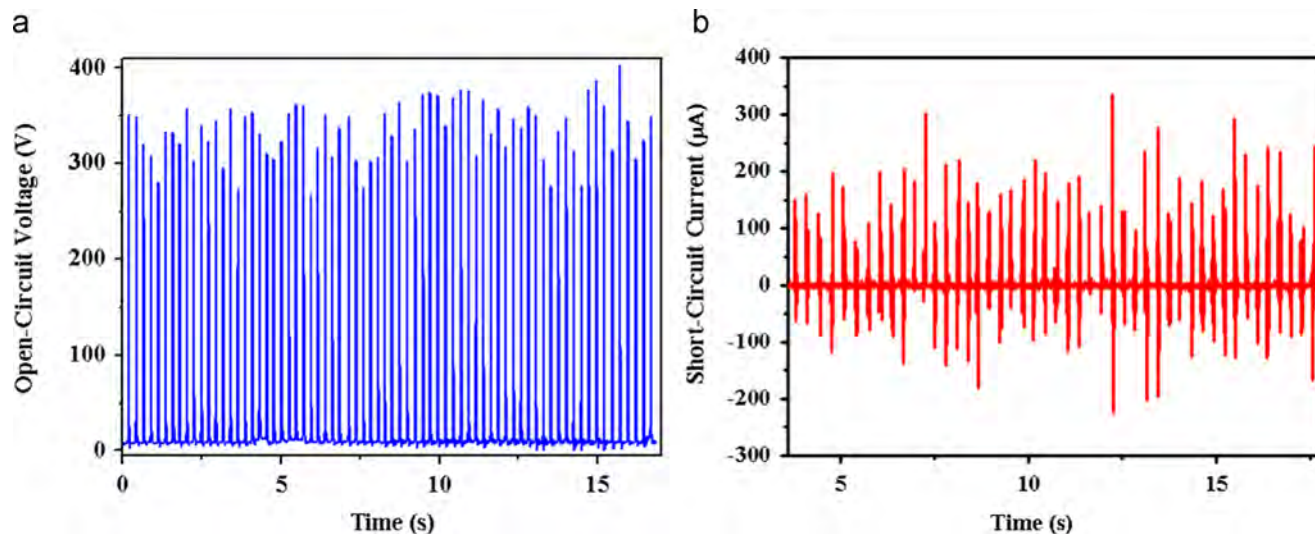


Figure 4 The performance of TENG for harvesting vibrational energy of human footfall. (a) Open-circuit voltage and (b) short-circuit current of TENG at footfall force of 500 N.

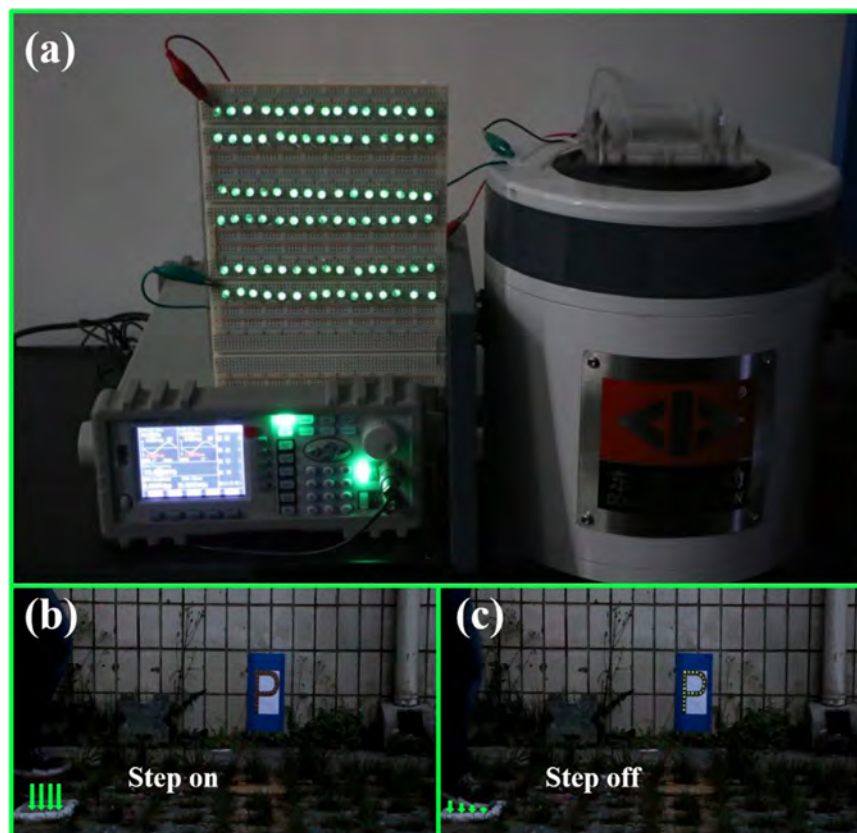


Figure 5 Demonstration of the PMNF-based TENG as a sustainable power source. (a) Photograph that shows TENG was working on an electrodynamic shaker at the resonance vibration frequency of 13.9 Hz. About 100 LEDs light up simultaneously. (b) Photograph of a setup in which the TENG acted as a direct power source for self-power pilot lamps and (c) when footstep fell on the TENG, simultaneously lighting up the pilot lamps in real time, promising a potential caution system of park or self-powered floor.

behavior. Moreover, the largest and smallest peaks are generated respectively with the process of the two contact surfaces moving apart after collision and approaching each other. The phenomenon that the peak value of short-circuit current is different in charge and discharge cycles, is normally resulting from the short-circuit current as a function of quantity of electricity and time (see Eq. (3)) while the same amount of charges are transferred back and forth when the two contact surfaces moving together and apart.

$$I = \frac{\Delta Q}{\Delta t} \quad (3)$$

To further investigate the output power of TENG at resonance frequency, resistors were provided as external loads. As displayed in Figure 3e, the instantaneous current amplitude drops with increasing load resistance owing to the resistive loss, while the voltage follows a build-up trend. Consequently, the instantaneous power ($W = I_{peak}^2 R$) peak at a load resistor of about $3 \text{ M}\Omega$, corresponding to a peak power density of about 9.28 W m^{-2} (Figure 3f).

To optimize the electrical output from the contact-separation behavior of TENG, an in-depth study was launched by means of footfall. At a force of about 500 N, this TENG can generate respectively V_{oc} up to 403 V and I_{sc} up to 0.34 mA (Figure 4a and b). The reason that the electrical output of footfall is bigger than vibration shaker is mainly due to the dramatically increased contact surface with the larger force (please see Figure S6, Supporting information).

Comparing to TENGs reported before, the TENG based wide-aperture PMNF with dual roles of positive electrode (Table 2, Supporting information) and its surface modification was first demonstrated to date. The high power output of TENG is mainly attributed to the following reasons: (i) the hybridization effect of both the contact-separation mode and sliding electrification mode (Figure S7, Supporting information) of flexible PDMS inserting into micropores of PMNF effectively enhanced the effective contact area and then the triboelectric charges of TENG due to the surface modifications of PMNF, which has been demonstrated by the contrastive data with the flat nickel plate (the detail is shown in Figures S8 and S9); (ii) the elastic property of PDMS which can easily deform in response to small pressure ensure as much contact area as it can be possibly obtained; (iii) the porous and rough surface of PMNF provides a bigger contact area.

To validate the capacity of harvesting mechanical energy in practical application, the as-grown TENG as a source was demonstrated to power electronic device (see Movie 2 and 3 in Supporting information). Figure 5a, this TENG was inspired by the vibration shaker system to harvest vibration energy at the resonance frequency of 13.9 Hz, lighting up simultaneously and continuously almost 100 light-emitting diode (LED) bulbs. Subsequently, as shown in Figure. 4b and c, the TENG was also excited by footfall to power a self-power indicator for stopping place (Figure 5a and b, Movie 3). The above results evidently show the tremendously potential applications for powering some wireless electronics by harvesting the vibration energy from highways, railways, and tunnels in remote mountain areas.

Supplementary material related to this article can be found online at <http://dx.doi.org/10.1016/j.nanoen.2015.06.012>.

Conclusions

In summary, we presented an innovative enhanced TENG based on a PMNF material with the positive polarity for some sustainably self-powered electronic devices by harvesting natural vibration mechanical energy. The working mechanism has been elaborated using the schematic drawing and finite-element simulation. The maximal short-circuit current and open-circuit voltage of as-prepared TENG reached up to $71.9 \mu\text{A}$ and 187.8 V at the resonance frequency of 13.9 Hz with the instantaneous power output of 9.3 mW and power density of 3.7 W/m^2 . Additionally, by the force of footfall, the TENG generated a bigger electric output up to 0.34 mA and 403 V. Therefore, due to the unique advantages of TENGs, such as porosity, cost-effectiveness, and light weight, this approach might open the possibility for obtaining green and sustainable energy from the ocean using the porous microstructured materials alike.

Experimental section

Preparation of nickel foam

As precious studies [48], the process to prepare the NI foam was divided into four step: (1) clean the organic matrix foam; (2) make this foam current conducting; (3) electroplated nickel metal on the foam; (4) eliminate the matrix foam with reductive sintering.

- i. *Clean the organic matrix foam.* The polyurethane sponge, used as the nickel foam matrix, was cleaned with a mixed solution of KMnO_4 and dilute H_2SO_4 . Subsequently, it was immersed in a reducing solution of oxalic acid and the washed in distilled water.
- ii. *Make this foam current conducting.* An alkaline hypophosphorous salt solution was employed as reductant to chemically electroplate the nickel. The concrete ingredient was $\text{NiSO}_4 \cdot 6\text{H}_2\text{O}$, $\text{Na}_4\text{P}_2\text{O}_7 \cdot 10\text{H}_2\text{O}$, $\text{NaH}_2\text{PO}_2 \cdot \text{H}_2\text{O}$ and distilled water, which was applied at about $30 \text{ }^\circ\text{C}$ with a pH of 10-11. A Ni-P alloy, $\sim 3 \mu\text{m}$ thick involving $\sim 5 \text{ wt}\%$ P, was forming and presenting greyish white metallic luster.
- iii. *Electroplate nickel metal on the foam.* A common electrodeposition was carried out with current density of $\sim 400 \text{ A m}^{-2}$. The electroplating time control the thickness of the nickel plating layer. The detailed component of the plating solution was $\text{NiSO}_4 \cdot 6\text{H}_2\text{O}$, NaCl , H_3BO_3 , Na_2SO_4 , MgSO_4 and H_2O , which was utilized at a temperature of $\sim 25 \text{ }^\circ\text{C}$ with a pH of 5.0-5.5.
- iv. *Eliminate the matrix foam with reductive sintering.* The organic matrix was burning at $600 \text{ }^\circ\text{C}$ for 4 min in air

oven. The organic foam and conductive agent will react with O₂ to form gaseous molecules, leaving nickel metal and NiO. And then a process that sinters the product at 850 °C with a reductive atmosphere of NH₃ for 40 min makes the NiO reduced to nickel metal.

Fabrication of the TENG

To construct the TENG, two pieces of acrylic sheets were prepared as substrates by a laser cutting machine with dimensions of 1.97 in. by 1.97 in. by 0.315 in. Four radius of 0.23 in. half-thorough grooves was drilled at each corner for spring installation. After the framework of the TENG was fabricated, aluminum foil was fixed on the top substrate as the back electrode. The colloidal PDMS, which was mixed by the PDMS elastomer and corresponding cross-linker in 10:1 ratio (w/w), was spin-coated on the aluminum foil of the top substrate at 500 rpm for 30 s. Then it was cured at 100 °C for 1 h in an oven. On the other acrylic substrate, nickel foam with a size of 1.97 in. × 1.97 in. × 0.04 in. which first acted as contact electrode was attached onto the bottom substrate. Subsequently, four springs (spring contact=3.58 lb/in.) was anchored to the top and bottom substrate together, leaving a parallel gap of 2 mm between the contact electrodes. Finally, lead wires were connected to the two contact electrodes for subsequent electrical measurement.

Measurement of the TENG

The output current signals of the triboelectric nanogenerator was measured by a low-noise current preamplifier (Stanford Research SR570). The output voltage signals of the triboelectric nanogenerator was measured by a low-noise voltage preamplifier (Keithley 6514 system electrometer).

Conflict of interest

The authors declare no competing financial interest.

Acknowledgments

This work is supported by the National Natural Science Foundation of China (No. 51202023), the scientific and technological projects for Distinguished Young Scholars of Sichuan Province (No. 2015JQ0013), the Fundamental Research Funds for the Central Universities of China (A0920502051408-10).

Appendix A. Supporting information

Supplementary data associated with this article can be found in the online version at <http://dx.doi.org/10.1016/j.nanoen.2015.06.012>.

References

- [1] R. Pelrine, R.D. Kornbluh, J. Eckerle, P. Jeuck, S. Oh, Q. Pei, S. Stanford, *Proc. SPIE*, 4329, 148-156.
- [2] P. Miao, P.D. Mitcheson, A.S. Holmes, E.M. Yeatman, T.C. Green, B.H. Stark, *Microsyst. Technol.* 12 (2006) 1079-1083.
- [3] P.D. Mitcheson, P. Miao, B.H. Stark, E.M. Yeatman, A. S. Holmes, T.C. Green, *Sens. Actuators A* 115 (2004) 523-529.
- [4] S.H. Wang, Y.N. Xie, S.M. Niu, L. Lin, C. Liu, Z.L. Wang, *Adv. Mater.* 26 (2014) 2818-2824.
- [5] S.H. Wang, L. Lin, Z.L. Wang, *Nano Energy* 11 (2015) 436-462.
- [6] Z.L. Wang, J.H. Song, *Science* 312 (2006) 242-246.
- [7] X.D. Wang, J.H. Song, J. Liu, Z.L. Wang, *Science* 316 (2007) 102-105.
- [8] Y. Qin, X. Wang, Z.L. Wang, *Nature* 451 (2008) 809-813.
- [9] R.S. Yang, Y. Qin, L.M. Dai, Z.L. Wang, *Nat. Nanotechnol.* 4 (2009) 34-39.
- [10] S. Xu, Y. Qin, C. Xu, Y.G. Wei, R.S. Yang, Z.L. Wang, *Nat. Nanotechnol.* 5 (2010) 366-373.
- [11] X.L. Bai, Y.M. Wen, J. Yang, P. Li, J. Qiu, Y. Zhu, *J. Appl. Phys.* 111 (2012) 07A938.
- [12] I. Sari, T. Balkan, H. Kulah, *Sens. Actuators A* 145-146 (2008) 405-413.
- [13] S.P. Beeby, R.N. Torah, M.J. Tudor, P. Glynn-Jones, T. O'Donnell, C.R. Saha, S. Roy, *J. Micromech. Microeng.* 17 (2007) 1257-1265.
- [14] L. Wang, F.G. Yuan, *Smart Mater. Struct.* 17 (2008) 045009.
- [15] S.P. Beeby, M.J. Tudor, N.M. White, *Meas. Sci. Technol.* 17 (2006) 175-195.
- [16] Z.L. Wang, *Sci. Am.* 298 (2008) 82-87.
- [17] Z.L. Wang, *Adv. Mater.* 24 (2011) 279-284.
- [18] R.J.M. Vullers, R.V. Schaijk, I. Doms, C.V. Hoof, R. Mertens, *Solid-State Electron.* 53 (2009) 684-693.
- [19] W. Yang, J. Chen, X. Wen, Q. Jing, J. Yang, Y. Su, G. Zhu, W. Wu, Z.L. Wang, *ACS Appl. Mater. Interfaces* 6 (2014) 7479-7484.
- [20] G. Zhu, W. Yang, T. Zhang, Q. Jing, J. Chen, Y.S. Zhong, P. Bai, Z.L. Wang, *Nano Lett.* 14 (2014) 3208-3213.
- [21] Y. Su, G. Zhu, W. Yang, J. Yang, J. Chen, Q. Jing, Z. Wu, Y. Jiang, Z. Wang, *ACS Nano* 8 (2014) 3843-3850.
- [22] X.N. Wen, W.Q. Yang, Y. Ding, S.M. Niu, Z.L. Wang, *Nano Res.* 7 (2014) 180-189.
- [23] J. Yang, J. Chen, Y. Liu, W. Yang, Y. Su, Z.L. Wang, *ACS Nano* 8 (2014) 2649-2657.
- [24] W. Yang, J. Chen, G. Zhu, J. Yang, P. Bai, Y. Su, Q. Jing, X. Chao, Z.L. Wang, *ACS Nano* 7 (2013) 11317-11324.
- [25] D. Shen, J.H. Park, J.H. Noh, S.Y. Choe, S.H. Kim, D.J. Kim, *Sens. Actuators A* 154 (2009) 103-108.
- [26] W. Yang, J. Chen, Q. Jing, J. Yang, X. Wen, Y. Su, G. Zhu, P. Bai, Z.L. Wang, *Adv. Funct. Mater.* 24 (2014) 4090-4096.
- [27] J. Chen, G. Zhu, W. Yang, Q. Jing, P. Bai, Y. Yang, T.C. Hou, Z. L. Wang, *Adv. Mater.* 25 (2013) 6094-6099.
- [28] G. Zhu, Z.H. Lin, Q.S. Jing, P. Bai, C.F. Pan, Y. Yang, Y.S. Zhou, Z.L. Wang, *Nano Lett.* 13 (2013) 847-853.
- [29] G. Zhu, C.F. Pan, W.X. Guo, C.Y. Chen, Y.S. Zhou, R.M. Yu, Z. L. Wang, *Nano Lett.* 12 (2012) 4960-4965.
- [30] S.H. Wang, L. Lin, Y.N. Xie, Q.S. Jing, S.M. Niu, Z.L. Wang, *Nano Lett.* 13 (2013) 2226-2233.
- [31] L. Lin, S.H. Wang, Y.N. Xie, Q.S. Jing, S.M. Niu, Y.F. Hu, Z. L. Wang, *Nano Lett.* 13 (2013) 2916-2923.
- [32] F.R. Fan, Z.Q. Tian, Z.L. Wang, *Nano Energy* 1 (2012) 328-334.
- [33] F.R. Fan, L. Lin, G. Zhu, W.Z. Wu, R. Zhang, Z.L. Wang, *Nano Lett.* 12 (2012) 3109-3114.
- [34] S.H. Wang, L. Lin, Z.L. Wang, *Nano Lett.* 12 (2012) 6339-6346.
- [35] J. Yang, J. Chen, Y. Yang, H. Zhang, W. Yang, P. Bai, Y. Su, Z. L. Wang, *Adv. Energy Mater.* 4 (2014) 1301322.
- [36] W. Yang, J. Chen, G. Zhu, X. Wen, P. Bai, Y. Su, Y. Lin, Z. L. Wang, *Nano Res.* 6 (2013) 880-886.
- [37] X.Y. Chen, M. Iwamoto, Z.M. Shi, L.M. Zhang, Z.L. Wang, *Adv. Funct. Mater.* 25 (2014) 739-747.
- [38] P. Bai, G. Zhu, Y.S. Zhou, S.H. Wang, J.S. Ma, G. Zhang, Z. L. Wang, *Nano Res.* 7 (2014) 990-997.

- [39] X.N. Wen, W.Q. Yang, Q.S. Jing, Z.L. Wang, *ACS Nano* 8 (2014) 7405-7412.
- [40] Q. Jing, G. Zhu, P. Bai, Y. Xie, J. Chen, R.P.S. Han, Z.L. Wang, *Nano Energy* 8 (2014) 3836-3842.
- [41] S.H. Wang, L. Lin, Y.N. Xie, Q.S. Jing, S.M. Niu, Z.L. Wang, *Nano Lett.* 13 (2013) 2226-2233.
- [42] G.S.P. Castle, *J. Electrostat.* 40-41 (1997) 13-20.
- [43] R.D. Kornbluh, R. Pelrine, H. Prahlah, A. Wong-Foy, B. McCoy, S. Kim, J. Eckerle, T. Low, *Proc. SPIE* 7976 (2011) 7976051.
- [44] G. Zhu, Y.J. Su, P. Bai, J. Chen, Q.S. Jing, W.Q. Yang, Z. L. Wang, *ACS Nano* 8 (2014) 6031-6037.
- [45] P.S. Liu, K.M. Liang, *Mater. Sci. Technol.* 16 (2000) 575-583.
- [46] E. Nemeth, V. Albrecht, G.F. Schubert, Simon, *J. Electrostat.* 58 (2003) 3-16.
- [47] R.V. Dukkupati, *Vibration Analysis*, Alpha Science International, Harrow, UK, 2004 Ch. 2.
- [48] L.H. Lee, *J. Electrostat.* 32 (1994) 1-29.



Lei Zhang received her B.E. degree in polymer material engineering from Chongqing University of Arts and Science in 2014. He is a graduate student in materials science and engineering at Southwest Jiaotong University under the guidance of Professor Weiqing Yang. His research focuses on the triboelectric nanogenerator and supercapacitor.



Long Jin received his B.E. from Southwest Jiaotong University in 2015. He is currently pursuing a master's degree in materials science and engineering at Southwest Jiaotong University under the guidance of Professor Weiqing Yang.



Binbin Zhang received his B.E. from Southwest Jiaotong University in 2015. He is currently pursuing a master's degree in materials science and engineering at Southwest Jiaotong University under the guidance of Professor Weiqing Yang.



Weili Deng received his B.S. degree in electronic science and technology from Chongqing University in 2006, and then earns his master degree in 2009. Now he is a doctor in materials science and engineering at Southwest Jiaotong University.



Hong Pan received her B.E. from Southwest University in 2014. She is graduate student in materials science and engineering at Southwest Jiaotong University under the guidance of Professor Weiqing Yang.



Junfeng Tang received his B.S. degree in metal material engineering from Chongqing University of Arts and Science in 2014. He is a graduate student in materials science and engineering at Southwest Jiaotong University now.



Minhao Zhu received his B.E. in metal materials science and engineering in 1990, M. S. in 1993, and PhD in 2001 from Southwest Jiaotong University. Now he is the professor of Southwest Jiaotong University, Yangtze River Scholar Distinguished Professor of China and National Outstanding Youth Fund Gainer. His current research focuses on Materials Science and Engineering, Mechanical Design and Theory.



Weiqing Yang received his M. S. in Physics in 2007, and PhD in Materials and Science Engineering from Sichuan University in 2011. He was a post-doctorate research fellow at University of Electronic Science and Technology of China from 2011 to 2013. Subsequently, he was a post-doctorate research fellow at Georgia Institute of Technology from 2013 to 2014, under the supervision of Prof. Zhonglin Wang. Now he joined Southwest Jiaotong University as a professor. His current research focuses on nano energy materials, micro-nano devices, and optoelectronic devices.